

## Elimination of Wnt Secretion From Stellate Cells Is Dispensable for Zonation and Development of Liver Fibrosis Following Hepatobiliary Injury

Rong Zhang,\*† Alexander T. Kikuchi,\*† Toshimasa Nakao,‡ Jacquelyn O. Russell,\*† Morgan E. Preziosi,\*† Minakshi Poddar,\*† Sucha Singh,\*† Aaron W. Bell,\*† Steven G. England,§ and Satdarshan P. Monga\*†¶

\*Department of Pathology, University of Pittsburgh,

School of Medicine and University of Pittsburgh Medical Center, Pittsburgh, PA, USA

†Pittsburgh Liver Research Center, University of Pittsburgh,

School of Medicine and University of Pittsburgh Medical Center, Pittsburgh, PA, USA

‡Department of Organ Transplantation and General Surgery, Graduate School of Medical Sciences,

Kyoto Prefectural University of Medical School, Hirokoji, Kawaramachi, Kamikyo-ku, Kyoto City, Kyoto, Japan

§Future Therapeutics and Technologies, Abbvie, North Chicago, IL, USA

¶Department of Medicine, University of Pittsburgh, School of Medicine and University of Pittsburgh Medical Center, Pittsburgh, PA, USA

Alterations in the Wnt signaling pathway including those impacting hepatic stellate cells (HSCs) have been implicated in liver fibrosis. In the current study, we first examined the expression of Wnt genes in human HSC (HHSCs) after treatment with a profibrogenic factor TGF- $\beta$ 1. Next, we generated HSC-specific Wntless (Wls) knockout (KO) using the *Lrat-cre* and *Wls*-floxed mice. KO and littermate controls (CON) were characterized for any basal phenotype and subjected to two liver fibrosis protocols. In vitro, TGF- $\beta$ 1 induced expression of Wnt2, 5a and 9a while decreasing Wnt2b, 3a, 4, and 11 in HHSC. In vivo, KO and CON mice were born at normal Mendelian ratio and lacked any overt phenotype. Loss of Wnt secretion from HSCs had no effect on liver weight and did not impact  $\beta$ -catenin activation in the pericentral hepatocytes. After 7 days of bile duct ligation (BDL), KO and CON showed comparable levels of serum alkaline phosphatase, alanine aminotransferase, aspartate aminotransferase, total and direct bilirubin. Comparable histology, Sirius red staining, and immunohistochemistry for  $\alpha$ -SMA, desmin, Ki-67, F4/80, and CD45 indicated similar proliferation, inflammation, and portal fibrosis in both groups. Biweekly administration of carbon tetrachloride for 4 or 8 weeks also led to comparable serum biochemistry, inflammation, and fibrosis in KO and CON. Specific Wnt genes were altered in HHSCs in response to TGF- $\beta$ 1; however, eliminating Wnt secretion from HSC did not impact basal  $\beta$ -catenin activation in normal liver nor did it alter the injury–repair response during development of liver fibrosis.

**Key words:** Wntless; Hepatic stellate cells (HSCs); Fibrosis; Cirrhosis; Animal model; Wnt; Myofibroblast; Transforming growth factor- $\beta$ 1 (TGF- $\beta$ 1); Platelet-derived growth factor (PDGF)

### INTRODUCTION

Hepatic fibrosis is a prolonged wound healing process regardless of its etiology, resulting from excessive accumulation of extracellular matrix (ECM) proteins<sup>1,2</sup>. Substantial evidence exists demonstrating that hepatic stellate cells (HSCs) are the main source of ECM production during hepatobiliary injury<sup>2–5</sup>. In response to liver injury, quiescent HSCs undergo activation into myofibroblasts featured by enhanced proliferation, migration, contraction, as well as altered, profibrotic and proinflammatory gene transcription<sup>2,3,6</sup>. Several signaling pathways are involved in the activation of HSCs; some are well

characterized, like platelet-derived growth factor (PDGF) and transforming growth factor- $\beta$  (TGF- $\beta$ ) signaling pathways<sup>2,7–9</sup>, whereas others are not so well elucidated, including Wnt signaling<sup>7,9,10</sup>.

Wnt signaling is crucial in liver pathophysiology including normal liver development and adult tissue homeostasis. Alterations in its activity are associated with development of hepatocellular carcinoma and other diseases<sup>10,11</sup>. One major role of Wnt/ $\beta$ -catenin signaling is regulating postnatal hepatic growth, which contributes to gain in liver weight (LW). Also, at baseline, Wnt/ $\beta$ -catenin signaling is active in pericentral hepatocytes

Address correspondence to Satdarshan P. S. Monga, M.D., FAASLD, Endowed Chair for Experimental Pathology, Professor of Pathology and Medicine (Gastroenterology, Hepatology and Nutrition), Assistant Dean and Co-Director: Medical Scientist Training Program, Program Director: CATER Training Program, Director: Pittsburgh Liver Research Center, University of Pittsburgh, School of Medicine, 200 Lothrop Street S-422 BST, Pittsburgh, PA 15261, USA. Tel: (412) 648-9966; Fax: (412) 648-1916; E-mail: [smonga@pitt.edu](mailto:smonga@pitt.edu)

and contributes to metabolic zonation. Lack of  $\beta$ -catenin or Wnt coreceptors leads to disruption of glutamine synthetase (GS) expression in zone 3 hepatocytes<sup>12-14</sup>. While endothelial cells lining the central vein are known to be a source of Wnt ligands that regulate zonation, and macrophages and hepatocytes have been ruled out as the source of Wnt ligands, the role of HSCs as source of Wnts for this process is unknown<sup>14-16</sup>.

Increased expression of Wnt pathway components was first reported in liver fibrosis by genetic analysis of primary biliary cirrhosis livers in 2001<sup>17,18</sup>. Following these observations, several investigations have attempted to address the role of Wnt signaling pathway in HSC activation and liver fibrosis. However, a consensus on the role of Wnt signaling in HSC biology remains ambiguous. One study demonstrated that Wnt/ $\beta$ -catenin pathway negatively regulates HSC activation<sup>19</sup>, while a growing body of publications support positive correlation between the activation of canonical Wnt signaling pathway and the process of HSC activation and fibrosis<sup>20-25</sup>. Simultaneously, noncanonical Wnt signaling ( $\beta$ -catenin independent) and its components have also been identified as contributors of HSC activation and as constituents of fibrotic livers<sup>26-31</sup>. A few studies have shown that in vitro and in vivo antagonism of the Wnt signaling pathway with an inhibitor of interactions between the CREB-binding protein (CBP) and  $\beta$ -catenin suppresses and even reverses the activation of HSCs to alleviate hepatic fibrogenesis<sup>20,22,27</sup>. These findings suggest a correlation between the activation of Wnt signaling pathway in activated HSCs and liver fibrosis. However, the source of Wnt ligands and whether they impact HSC biology in an autocrine or a paracrine manner, along with the role of HSC as source of Wnts in hepatic fibrosis, has not been investigated.

In order to directly address the relevance of HSC as a source of Wnt signaling and its impact on hepatic fibrosis, we generated HSC-specific Wntless (Wls) knockout (KO) mice by breeding previously described Wls-floxed mice and lecithin retinol acyl transferase (LRAT)-driven Cre (Lrat-cre) transgenic mice<sup>5</sup>. Wls is an obligate chaperone protein required for Wnt secretion in all cells; therefore, these KO mice are unable to secrete any Wnt proteins from HSCs, thereby providing an opportunity for us to examine the role of any Wnt ligand secreted from HSCs in the baseline liver as well as in development of injury and fibrosis.

## MATERIALS AND METHODS

### *Generation of HSC-Specific Wntless Knockout Mice*

Lrat-cre mice (C57BL/6 strain), described previously, were kindly provided by Dr. Robert Schwabe<sup>5</sup>. To generate HSC-specific Wls-knockout mice (KO), homozygous

floxed Wls mice (Wls<sup>loxp/loxp</sup>) were bred to the Lrat-cre mice (Lrat-cre<sup>+/-</sup>), and offspring carrying one floxed Wls allele and Lrat-cre allele were then crossed to Wls<sup>loxp/loxp</sup> mice. The resulting mice with genotype Wls<sup>loxp/loxp</sup>; Lrat-cre<sup>+/-</sup> are referred henceforth as KO, and littermates with genotypes Wls<sup>loxp/loxp</sup>; Lrat-cre<sup>-/-</sup> or Wls<sup>loxp/WT</sup>; Lrat-cre<sup>-/-</sup> as controls (CON). To validate efficacy of Lrat-cre in conditionally deleting floxed genes in HSCs, we bred the ROSA26-Stop<sup>flox/flox</sup>-EYFP mice with Wls<sup>loxp/loxp</sup>; Lrat-cre<sup>+/-</sup> KO mice.

### *Liver Fibrosis and Injury Models*

Liver fibrosis was induced by intraperitoneal (IP) injections of 0.5  $\mu$ l CCl<sub>4</sub> per gram body weight (BW), dissolved in corn oil at a ratio of 1:3, twice a week for 4 or 8 weeks. Cholestatic liver fibrosis was induced by common bile duct ligation for 7 days.

### *Isolation of Hepatic Stellate Cells*

Primary HSCs were isolated via in situ collagenase perfusion of the liver, removal of hepatocytes and debris by low speed centrifugation, followed by Nycodenz (Accurate Chemical) density gradient centrifugation as described previously<sup>32</sup>. HSCs were then extracted with TRIzol (Thermo Fisher Scientific, Waltham, MA, USA) as per manufacturer's instructions for RNA, DNA, and protein analyses.

### *Cell Culture*

Cell culture and TGF- $\beta$ 1 treatment of human HSCs (HHSCs) were described previously<sup>33</sup>. Briefly, HHSCs (Cat. No. 5300) were purchased twice from ScienCell Research Laboratories (Carlsbad, CA, USA) and cultured according to the protocol provided by the company. Cells were used prior to 6th passage and serum starved 12 h prior to treatment by washing cells twice with sterile, cold PBS followed by addition of serum-free Stellate Cell Medium (ScienCell) containing recombinant TGF- $\beta$ 1 (2 ng/ml; R&D Systems) for 24 h before harvesting the cells for RNA and qPCR analysis.

### *Histology, Immunohistochemistry, and Immunofluorescence*

Liver specimens were fixed in 10% buffered formalin and embedded in paraffin. Hematoxylin and eosin (H&E) staining on 4- $\mu$ m liver sections was performed. Immunohistochemistry was performed on these sections as described below. Briefly, deparaffinized sections were incubated in 3% H<sub>2</sub>O<sub>2</sub> dissolved in 1 $\times$  phosphate-buffered saline (PBS) for 10 min to quench the endogenous peroxidase. Slides were pressure cooked in antigen retrieval buffer for 20 min. Subsequently, slides were incubated with primary antibodies overnight at 4°C. Primary antibodies used in the study include Ki-67 (NM-sP6; Thermo Fisher Scientific), GS (SC-74430; Santa Cruz Biotechnology),

desmin (NB120-15200, Novus Biologicals),  $\beta$ -catenin (610514, BD), PCNA (sc-56, Santa Cruz Biotechnology), CD45 (sc-53665, Santa Cruz Biotechnology), F4/80 (MCA497GA, Bio-Rad), and  $\alpha$ -smooth muscle actin ( $\alpha$ -SMA) (ab5694, Abcam). After washes, the sections were incubated in the appropriate biotin-conjugated secondary antibody (Chemicon, Temecula, CA, USA) for 30 min at room temperature. Signal was detected using the Vectastain ABC Elite kit (Vector Laboratories, Inc., Burlingame, CA, USA) and developed using DAB (Vector Laboratories, Inc.). Sections were counterstained with Shandon hematoxylin solution (Thermo Fisher Scientific, Pittsburgh, PA, USA), subjected to dehydration process and coverslipped. For negative control, sections were incubated with secondary antibodies only or with control IgG.

#### Immunofluorescence Staining

Samples were fixed in 10% buffered formalin overnight, transferred to 30% sucrose in PBS and incubated at 4°C overnight, then frozen in OCT compound (4583; Sakura) at -80°C. Livers were cut into 5- $\mu$ m sections and allowed to air dry. Next, sections were washed in PBS and microwaved in preheated sodium citrate buffer (pH 6) for 6 min twice (12 min total, evaporated buffer was

replaced after 6 min in the microwave). After cooling, slides were washed in PBS, permeabilized in 0.1% Triton X-100 in PBS for 20 min, and washed with PBS three times. Sections were then blocked with 2% goat serum in PBS with 0.1% Tween<sup>®</sup>-20 (antibody diluent) for 30 min at room temperature (RT). Primary antibodies for desmin (Novus, NB120-15200) and GFP (Abcam, ab13970) were diluted 1:200 in antibody diluent and applied to the samples overnight at 4°C. Sections were next washed in PBS for 5 min three times. Secondary antibodies Alexa Fluor<sup>®</sup> 488 goat anti-rabbit (A11008; Life Technologies, Carlsbad, CA, USA) and 555 goat anti-chicken (A21437; Life Technologies) were diluted 1:400 in antibody diluent and incubated at RT for 3 h. Samples were washed in PBS for 5 min three times, treated with 1 mg/100 ml DAPI (B2883; Sigma-Aldrich) in distilled water for 1 min, and washed with PBS three times. Coverslips were applied with ProLong<sup>™</sup> Gold antifade reagent (P10144; Invitrogen), and samples were imaged on a Nikon Eclipse Ti epifluorescence microscope.

#### Protein Extraction and Western Blot

Liver tissues were homogenized in lysis buffer [30 mM Tris (pH 7.5), 150 mM NaCl, 1% NP-40, 0.5%

**Table 1.** Real-Time PCR Primers Used in This Study

Gene	Forward Primer	Reverse Primer
cDNA primers		
Human Wnt2	TAGTCGGGAATCTGCCTTTG	TTCCTTTCCTTTGCATCCAC
Human Wnt2b	TGCCAAGGAGAAGAGGCTTAAG	GTGCGACCACAGCGTTTAT
Human Wnt3	GGAGAAGCGGAAGGAAAAATG	GCACGTCGTAGATGCGAATACA
Human Wnt3a	CCTGCACTCCATCCAGCTACA	GACCTCTCTTCTACCTTTCCCTTA
Human Wnt4	GATGTGCGGGAGAGAAGCAA	ATTCCACCCGCATGTGTGT
Human Wnt5a	GAAATGCGTGTGGGTTGAA	ATGCCCTCTCCACAAAGTGAA
Human Wnt5b	CTGCCTTCCAGCGAGAATT	AGGTCAAATGGCCCCCTTT
Human Wnt6	GGTTATGGACCCTACCAGCA	AATGTCCTGTTGCAGGATGC
Human Wnt7a	AGTACAACGAGGCCGTTTCCAC	GCACGTGTTGCACTTGACAT
Human Wnt7b	CCCGGAACCTTCTCTTTCTTC	GGCGTAGCTTTTCTGTGTCCAT
Human Wnt8a	TGGGGAACCTGTTTATGCTC	CCCTCGGCTTGGTTGTAGTA
Human Wnt8b	GACAATGTGGCTTCGGAGA	GAGTGCTGCGTGGTACTTCT
Human Wnt9a	CTTAAGTACAGCAGCAAGTTCGTC	CCACGAGTTGTTGTGGAAAGT
Human Wnt9b	CAGGTGCTGAACTGCGCTAT	GCCCAAGGCCTCATTGGT
Human Wnt10a	GGCAACCCGTCAGTCTGTCT	CATTCCCCACCTCCCATCT
Human Wnt10b	CTTTTAGCCCTTTGCTCTGAT	CCCCTAAAGCTGTTTCCAGGTA
Human Wnt11	TTGCTTGACCTGGAGAGAGG	GACGAGTTCCGAGTCCCTTCA
Human Wnt16	TGCTCCGATGATGTCCAGTA	ACCTCCTGCAACGGACATAG
Human Wls	TATCTGGACTACAGACATTGG	CTTCCGTTACCTGACTAACG
m-PCDH7	TCCACTCCCAGAGGACAACCT	GGCTGGCTCTTCTTCCCTCTC
m-Desmin	GTGAAGATGGCCTTGGATGT	CGGGTCTCAATGGTCTTGAT
m-Lrat	CTCTCGGATCAGTCCACAGG	ATCCCAAGACAGCCGAAGC
m-Wls	TTGTATGCACCATCCCATAAGA	GCTGTGGACACCCAGGTC
m-Cyclophilin A	CCCCACCGTGTCTTCGACA	TCCAGTGCTCAGAGCTCGAAA
gDNA primer		
WLS-FLOX DEL	CTTCCCTGCTTCTTTAAGCGTC	CTCAGAACTCCCTTCTTGAAGC

Na deoxycholate, 0.1% SDS] containing the Complete Protease and Phosphatase Inhibitor Cocktail (Roche Molecular Biochemicals). Protein concentration was determined with the Bio-Rad Protein Assay Kit (Bio-Rad, Hercules, CA, USA) using bovine serum albumin as a standard. Aliquots of 30- g proteins were denatured by boiling in Tris-Glycine SDS Sample Buffer (Life Technologies), resolved by SDS PAGE, and transferred to nitrocellulose membranes (Bio-Rad, Hercules, CA, USA) using the Bio-Rad transfer apparatus. Membranes were blocked in 5% BSA in Tris-buffered saline containing 0.1% Tween 20 for 1 h and probed with primary antibodies. Primary antibodies used in the study include PDGFR (cs3174; Cell Signaling Technology), PDGFR (cs3169; Cell Signaling Technology),  $\alpha$ -SMA (a2547; Sigma-Aldrich), and desmin (NB120-15200; Novus Biologicals). Each primary antibody was followed by incubation with horseradish peroxidase secondary antibody diluted 1:10,000 for 1 h. After appropriate washing, the signal was developed with the Super Signal West Pico or Super Signal West Femto (Thermo Fisher Scientific, Waltham, MA, USA).

#### Real-Time PCR

RNA was extracted from adherent cell cultures using Direct-zol RNA MiniPrep Plus kit (Zymo Research, Irvine, CA, USA) following the manufacturer's protocol. RNA (1 g) from each sample was used to make individual cDNA with SuperScript III First-Strand Synthesis System for RT-PCR (Invitrogen). cDNA along with 1 $\times$  Power SYBR-Green PCR Master Mix (Applied Biosystems) and the appropriate primers (Table 1) were used for each real-time PCR reaction with Applied Biosystems StepOnePlus Real-Time PCR System. The comparative CT method was used for analysis of data.

#### Quantification of Immunohistochemistry (IHC) Images

Bright-field images of IHC staining were split into hematoxylin and DAB channels by Color Deconvolution using ImageJ Fiji (<https://imagej.net/Welcome>). The DAB staining in DAB channel of each antibody was highlighted with appropriate threshold; then the percentage of area of the DAB staining to the total image was measured.

#### Statistical Analysis

All experiments were performed with four to five animals in each group. Where applicable all data are presented as mean  $\pm$  standard deviation (SD). Statistical differences among the various groups were assessed with Welch's *t*-test, and *p* values ( $p < 0.05$ ,  $p < 0.01$ ,  $p < 0.005$ , and  $p < 0.0001$ ) were considered statistically significant. All statistics were performed with Prism 6, version 7.0 (GraphPad Software Inc., La Jolla, CA, USA).

## RESULTS

### Characterization of Expression of WNT Ligands in Primary HHSCs

Changes in mRNA expression of several Wnt genes were examined in primary HHSCs after exposure to TGF- $\beta$ 1 as described in Materials and Methods. Wnt2b, Wnt3, Wnt3a, Wnt4, Wnt5b, Wnt9b, Wnt10a, Wnt10b, and Wnt11 were significantly downregulated in the HHSCs after 24 h of TGF- $\beta$ 1 treatment compared to controls (Fig. 1A). A significant increase in the expression of Wnt2, Wnt5a, and Wnt9a was observed after TGF- $\beta$ 1 treatment of HHSCs (Fig. 1B). Finally, Wls mRNA was assessed and found to be significantly decreased with TGF- $\beta$ 1 treatment (Fig. 1C). Thus, a known profibrogenic factor altered the expression of several Wnts in HHSCs.

### Conditional Deletion of Wls From HSC Does Not Impact Pericentral $\beta$ -Catenin Activation or Lead to Any Other Overt Phenotype

Although the efficacy of Lrat-cre to target HSCs has been unequivocally demonstrated elsewhere, we validated its effectiveness in our own laboratory by crossing ROSA26-Stop<sup>fllox/fllox</sup>-EYFP mice with Lrat-cre mice<sup>5</sup>.

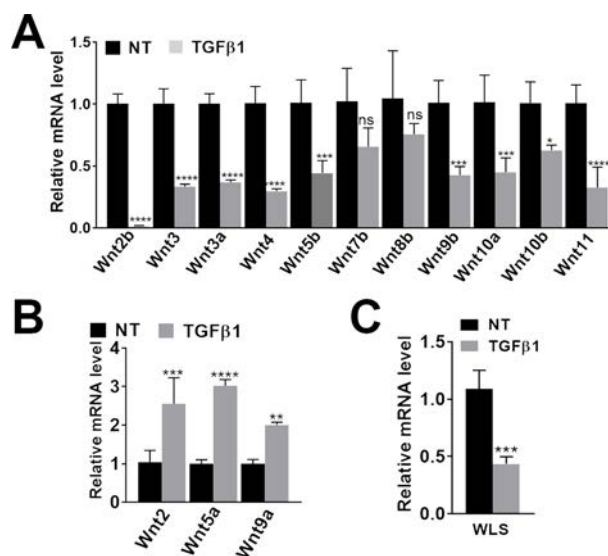


**Figure 1.** Effect of profibrogenic factor on Wnt gene expression in human hepatic stellate cells (HHSCs). HHSCs (ScienCell) were treated with TGF- $\beta$ 1 in triplicates, and the experiment was repeated with two different batches of cells. A representative analysis is shown. (A) Significant downregulation of several Wnt genes in transforming growth factor- $\beta$ 1 (TGF- $\beta$ 1)-treated HHSCs compared to nontreated (NT) cells in basal media for 24 h. (B) Significant increase in Wnt2, Wnt5a, and Wnt9a after TGF- $\beta$ 1 treatment. (C) Significant decrease in Wls expression was observed after TGF- $\beta$ 1 treatment. ns, not significant. \* $p < 0.05$ ; \*\* $p < 0.01$ ; \*\*\* $p < 0.005$ ; \*\*\*\* $p < 0.0001$ ; Welch's *t*-test.

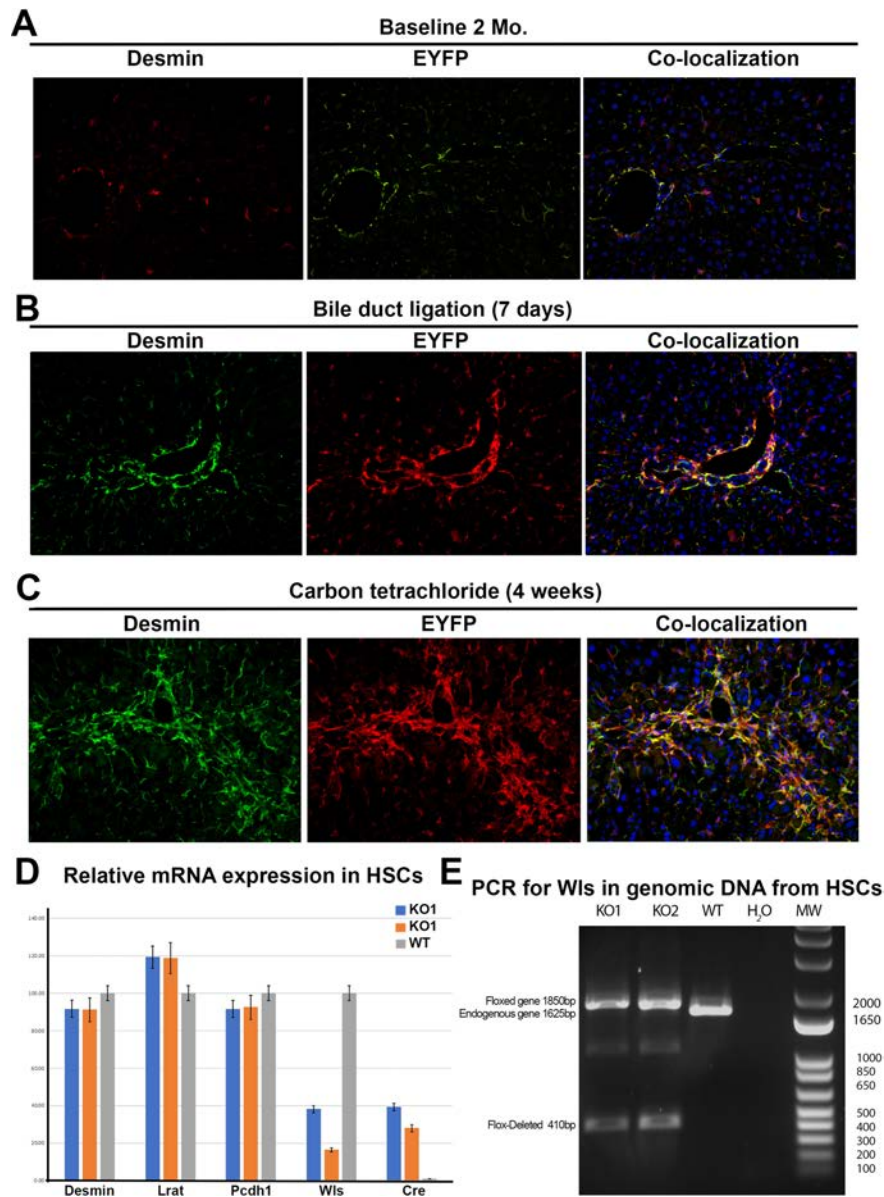


**Figure 2.** Lecithin retinol acyl transferase (LRAT)-driven Cre (Lrat-cre) induces successful recombination of floxed genes in the stellate cells at baseline and in activated myofibroblasts after bile duct ligation (BDL) and CCl<sub>4</sub> exposure. Male Rosa26-Stop<sup>flox/flox</sup>-EYFP:Wls<sup>flox/flox</sup> mice were bred to female Lrat-cre mice, and mice carrying Lrat-cre allele ( $n=3$ ) was assessed at baseline. HSCs isolated from these mice ( $n=2$ ) were also isolated from these mice to perform genomic DNA PCR and qRT-PCR analysis compared to HSCs from the littermate wild-type (WT) control mice. Further, as a proof of concept, Rosa26-Stop<sup>flox/flox</sup>-EYFP:PDGFR<sup>flox/flox</sup> mice were bred to female Lrat-cre mice, and mice carrying Lrat-cre allele in the progeny were subjected to BDL for 7 days ( $n=3$ ) or biweekly injections of CCl<sub>4</sub> for 4 weeks ( $n=3$ ) at which time mice were euthanized and livers processed by confocal immunofluorescence for any colocalization of desmin (marker of HSC) and EYFP (marker of cellular Lrat-cre activation). (A) Predominant desmin<sup>+</sup> cells coexpress EYFP at baseline in 2-month-old mice, indicating Lrat-cre activation in HSC at this time (200 $\times$ ). (B) Predominant desmin<sup>+</sup> cells coexpress EYFP at 7 days after BDL indicating Lrat-cre activation in HSC at this time (200 $\times$ ). (C) Predominant desmin<sup>+</sup> cells also coexpress EYFP at 4 weeks after CCl<sub>4</sub> demonstrating activation of Lrat-cre in HSC at this time in this model (200 $\times$ ). (D) Graphical representation of relative mRNA expression in isolated primary HSCs from KO and wild-type mice. Desmin, Lrat, and Pcdh7 are equally expressed in KO and wild-type cells indicating equivocal HSC enrichment. Wls mRNA is greatly diminished in the male (KO-1) and female (KO-2) cells relative to wild type. Remnant Wls expression can be attributed to contaminating cells in the HSC prep. Cre mRNA expression was detected only in the KO HSC samples. (E) Agarose gel electrophoresis of genomic DNA PCR products from purified primary HSCs using primers to detect Wls-flox deletion. Endogenous WLS allele (1,625 bp) is evident only in WT HSCs. Floxed Wls allele (1,850 bp) is evident in the KO1 (male) and KO2 (female) purified cells, which indicates nondeleted alleles from other non-HSC-contaminating liver cells. Flox-deleted allele (410 bp) is evident in only the KO HSCs, indicating successful genomic deletion by Lrat-cre.

At baseline in 8-week-old mice, or after 7 days of BDL or 4 weeks of CCl<sub>4</sub> administration, there was a clear colocalization of EYFP with desmin, validating the efficiency of Lrat-cre in eliminating floxed genes in HSCs in these KO mice and in two models of fibrosis (Fig. 2A–C). Furthermore, we isolated primary HSCs from KO and wild-type mice and examined mRNA expression of HSC marker genes as well as Cre recombinase. Cre mRNA expression was evident in the HSCs from KO mice at

baseline but not in wild-type HSCs (Fig. 2D). HSC marker genes, desmin, Lrat, and Pcdh7, were equivalently expressed in both WT and KO HSCs; however, Wls mRNA expression was markedly reduced in the KO HSCs. In addition, we analyzed genomic DNA from isolated HSCs of WT and KO mice using primers to detect the null allele. DNA PCR analysis reveals that the genetic deletion of the floxed exon-1 sequence is evident in KO HSCs at baseline (Fig. 2E).

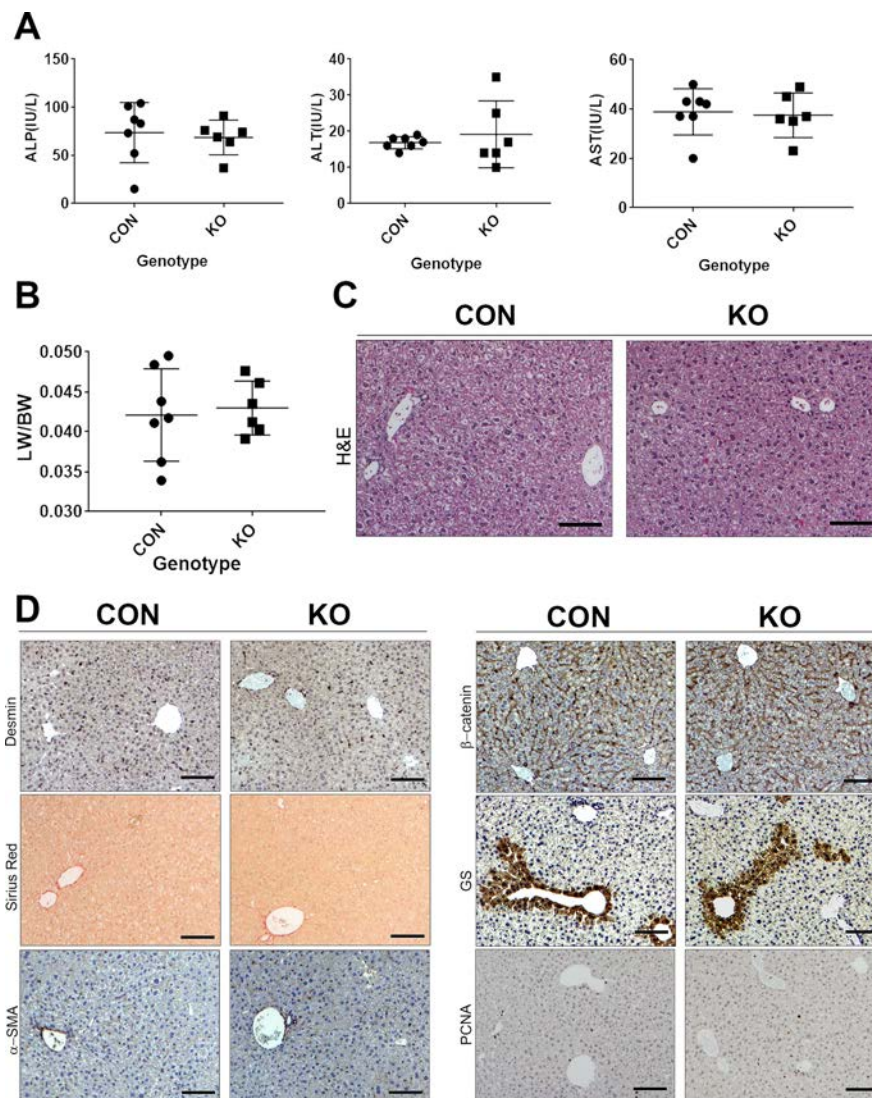


**Figure 3.** Baseline characterization of KO ( $n=6$ ) that lack Wls in HSCs and hence Wnt-secreting ability from HSC compared to littermate CON ( $n=7$ ). (A) Serum biochemistry from baseline KO and CON mice showing lack of any basal alterations in ALP, ALT, and AST. (B) No significant difference in liver weight-to-body weight ratio (LW/BW) was observed between the two groups. (C) Hematoxylin and eosin (H&E) staining on liver sections from representative CON and KO showed normal and comparable histology. Scale bar: 100  $\mu$ m. (D) Lack of differences in the number of HSCs as shown by staining for desmin or activation of HSCs as shown by lack of staining for  $\alpha$ -SMA or presence of fibrosis, as assessed by Sirius red staining in representative sections from KO and CON. Also, comparable membranous staining for  $\beta$ -catenin and lack of any alteration in its pericentral hepatocyte target glutamine synthetase (GS) in KO and CON demonstrates no discernible difference in Wnt signaling at baseline. Only occasional PCNA<sup>+</sup> hepatocytes were evident in representative staining of KO and CON livers. Scale bar: 100  $\mu$ m.

To determine the role of HSCs as a source of Wnt secretion in normal liver pathophysiology, we further analyzed the *Lrat-cre:Wls* KO mice. The CON and KO mice were born at normal Mendelian ratios and without any overt phenotypes. Examination of serum biochemistry for ALP, ALT, and AST did not show significant differences between the KO and CON (Fig. 3A). No difference in the LW/BW was evident between the two groups (Fig. 3B). H&E staining on liver sections from both the CON and KO showed normal and comparable histology without any evidence of basal fibrosis or inflammation (Fig. 3C). To identify the existence of any differences in the number of HSCs, activation of HSCs, or presence of fibrosis, we assessed KO and CON liver sections for desmin,  $\alpha$ -SMA, and Sirius red staining for collagen. Comparable immunohistochemical staining for both desmin and  $\alpha$ -SMA as well as minimal normal staining with Sirius red restricted to areas of the central vein or portal triad was observed in CON and KO (Fig. 3D).

As  $\beta$ -catenin activation is known to occur in pericentral hepatocytes at baseline as part of metabolic zonation,

we wanted to next address if HSCs could be the source of Wnts dictating this process. We did not observe any change in basal  $\beta$ -catenin activation in hepatocytes as seen by predominantly membranous  $\beta$ -catenin in both CON and KO livers as well as normal GS staining in the pericentral hepatocytes in both groups (Fig. 3D).

Although there was no difference in LW/BW, we wanted to directly address if there was any difference in hepatocyte proliferation because of lack of Wnt secretion from HSCs at baseline. Occasional but comparable numbers of PCNA<sup>+</sup> hepatocytes were evident in both groups at baseline (Fig. 3D).

Based on all the above analyses, we conclude that removal of Wls from HSCs results in no overt phenotype in these mice at baseline.

*KO Mice Respond to BDL Akin to CON*

To determine the role of HSCs in secreting Wnts during portal fibrosis, we subjected CON and KO mice to BDL for 7 days (Fig. 4A). Serum biochemistry analysis of CON and KO mice showed similar results for ALP, ALT, AST, direct BR, and total BR (Fig. 4B). H&E

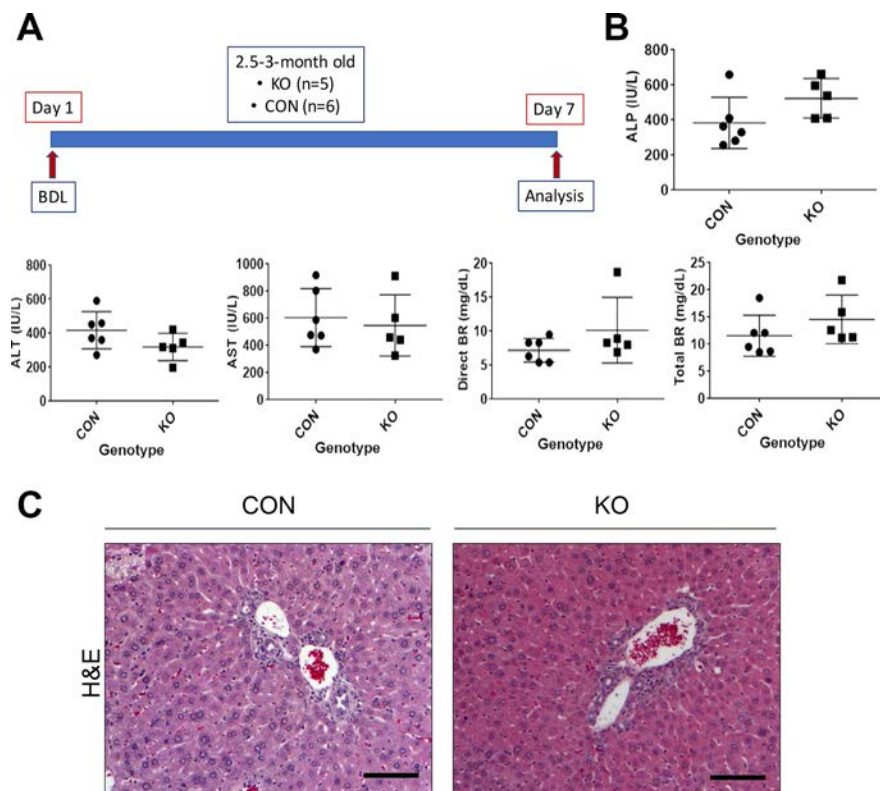


**Figure 4.** KO and CON mice subjected to BDL for 7 days show comparable biochemical injury and histology. (A) Schematic showing age- and sex-matched 2.5- to 3-month old KO ( $n=5$ ) and CON ( $n=6$ ) subjected to 7 days of BDL at which time they were euthanized for serum and liver analysis. (B) Serum biochemistry shows expected abnormally high values of ALP, ALT, AST, direct BR, and total BR at 7 days after BDL, although differences between KO and CON were insignificant. (C) H&E staining showed remarkable ductular reaction and periportal immune cell infiltration in both CON and KO at 7 days after BDL. Scale bar: 100  $\mu$ m.

staining showed remarkable ductular reaction and periportal immune cell infiltration in both CON and KO. Immunohistochemistry for Ki-67 to identify cells in the S phase as a marker of proliferation showed clusters of proliferating cells especially in the periportal regions in both CON and KO (Fig. 5). IHC for CD45, a leukocyte marker, manifested a common pattern of periportal distribution in both KO and CON (Fig. 5). Likewise, staining for the macrophage marker F4/80 was also comparable between the KO and CON (Fig. 5).

Next, we directly assessed the wound healing response in the KO versus CON following BDL. In response to BDL-induced injury and inflammation, liver accumulates activated collagen-producing myofibroblasts. KO and CON displayed comparable desmin and  $\alpha$ -SMA staining after 7 days of BDL both by IHC and by Western blot (Fig. 6A and B). This implies comparable activation of myofibroblasts in KO and CON and was further verified by comparable Sirius red staining (Fig. 6A). Both PDGFR<sup>34,35</sup> and PDGFR<sup>7,8</sup> are expressed in activated myofibroblasts and are critical mediators of liver fibrosis. Western blot results showed that both PDGFR and PDGFR were modestly decreased in KO compared to CON at 7 days after BDL (Fig. 6B). Thus, taken together, our data suggest that Wls loss from HSC, which prevents secretion of any Wnt ligand from these cells, does not

alter the process of hepatobiliary injury and fibrosis after BDL in any profound manner.

#### *KO and CON Mice Show Similar Injury and Fibrosis After 4 or 8 Weeks of CCl<sub>4</sub> Administration*

Next, we subjected CON and KO mice to another fibrosis model induced by biweekly injections of CCl<sub>4</sub> for 4 or 8 weeks (Fig. 7A). The LW/BW in KO was comparable to the CON at both 4 and 8 weeks after CCl<sub>4</sub> treatment (Fig. 7B and C). Serum ALP, AST, and ALT levels in animals 4 days after the last CCl<sub>4</sub> injection revealed insignificant differences between KO and CON at both 4 and 8 weeks (Fig. 7D and E). A more detailed histological characterization was then performed on tissue sections from KO and CON at both time points.

H&E staining at 4 weeks after CCl<sub>4</sub> showed some inflammation, fibrosis, and necrosis, which was comparable in KO and CON (Fig. 8). IHC for PCNA exhibited comparable numbers of proliferating hepatocyte cells in both groups (Fig. 8). IHC for CD45 and F4/80 also showed notable but comparable inflammation and macrophage infiltration in both groups at this time (Fig. 8). Quantification of all these immunohistochemical stains verified insignificant differences between the two groups (Fig. 8). We next investigated the extent of fibrosis, numbers of HSCs, and activated myofibroblasts by Sirius red

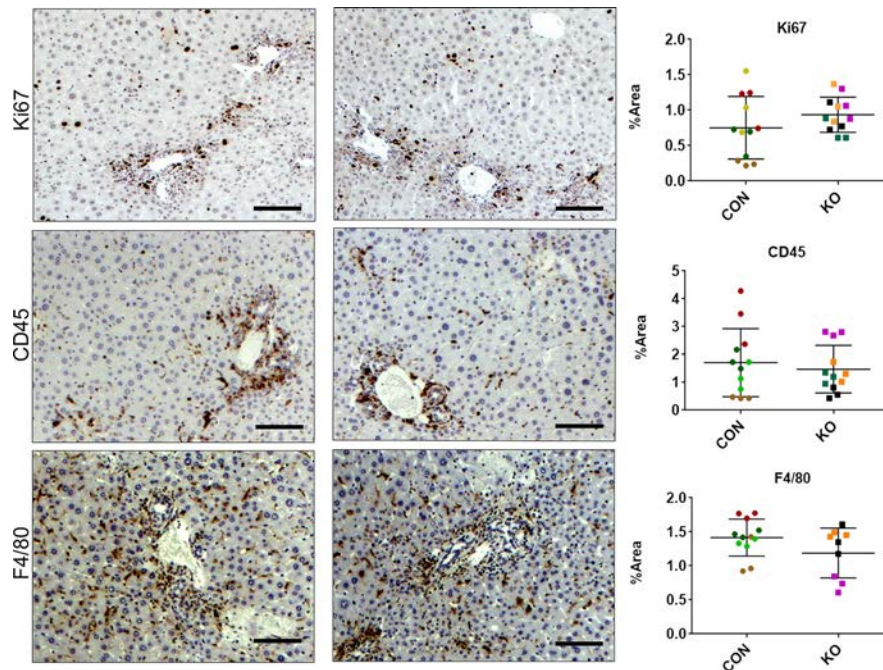


**Figure 5.** KO and CON mice subjected to BDL for 7 days show comparable histological repair, injury, and inflammation. Representative sections from KO and CON after 7 days of BDL show comparable immunostaining for Ki-67, CD45, and F4/80 showing comparable hepatocytes in the S phase of the cell cycle, comparable periportal immune response, and similar numbers and distribution of macrophages, respectively. Quantification of each of these stains verified lack of significant differences between the two groups for any of these markers. Scale bar: 100  $\mu$ m.

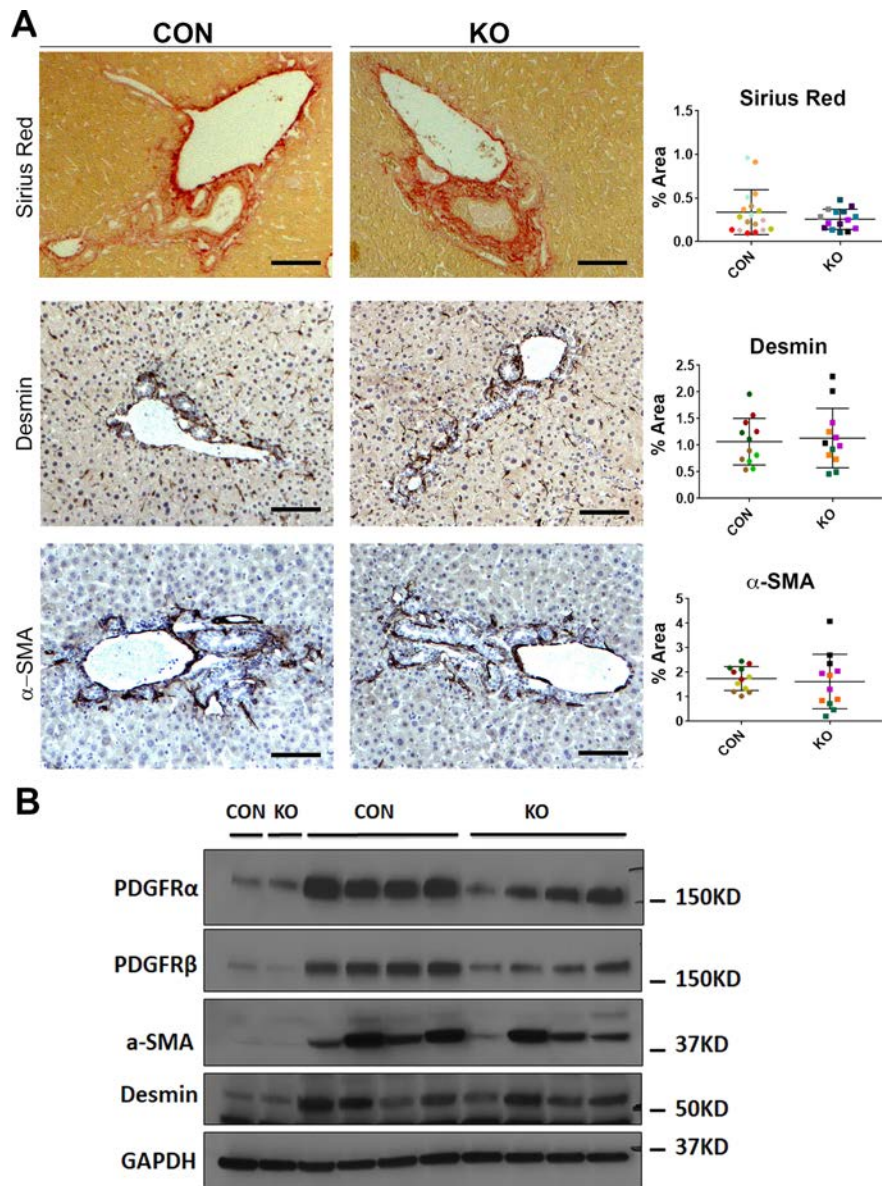


**Figure 6.** KO and CON mice subjected to BDL for 7 days show comparable activation of myfibroblasts and extent of periportal fibrosis. (A) Representative sections from KO and CON after 7 days of BDL show comparable Sirius red staining as well as immunostaining for desmin and  $\alpha$ -SMA indicating equivalent fibrosis, number of HSCs, and activated myfibroblasts. Quantification of each of these stains verified lack of significant differences between the two groups for any of these markers. Scale bar: 100  $\mu$ m. (B) Representative Western blot for markers of fibrosis showed comparably higher albeit somewhat variable desmin and  $\alpha$ -SMA levels in KO and CON after 7 days of BDL compared to their respective baseline controls. Interestingly, a modest decrease in PDGFR  $\alpha$  and PDGFR  $\beta$  levels was observed in KO after 7 days of BDL compared to those of controls, despite lack of notable changes in overall fibrosis. GAPDH was used as loading control.

staining, and immunostaining for desmin and  $\alpha$ -SMA, respectively. KO livers displayed Sirius red staining comparable to the CON livers at 4 weeks of CCl<sub>4</sub> treatment (Fig. 9A). Likewise, IHC staining for desmin and  $\alpha$ -SMA was similarly high between KO and CON livers after 4 weeks of CCl<sub>4</sub> (Fig. 9A). Western blot analysis for desmin,  $\alpha$ -SMA, as well as other markers of hepatic fibrosis including PDGFR  $\alpha$  and PDGFR  $\beta$  were similarly

increased over their respective baseline in both CON and KO at 4 weeks of CCl<sub>4</sub> treatment (Fig. 9B). Taken together, these data imply that loss of all Wnt secretion from HSCs does not affect the process of injury recovery and fibrosis after 4-week CCl<sub>4</sub> administration.

We then assessed the histology, proliferation, inflammation, and fibrosis in KO and CON mice challenged with CCl<sub>4</sub> injection for 8 weeks. IHC analysis of PCNA,

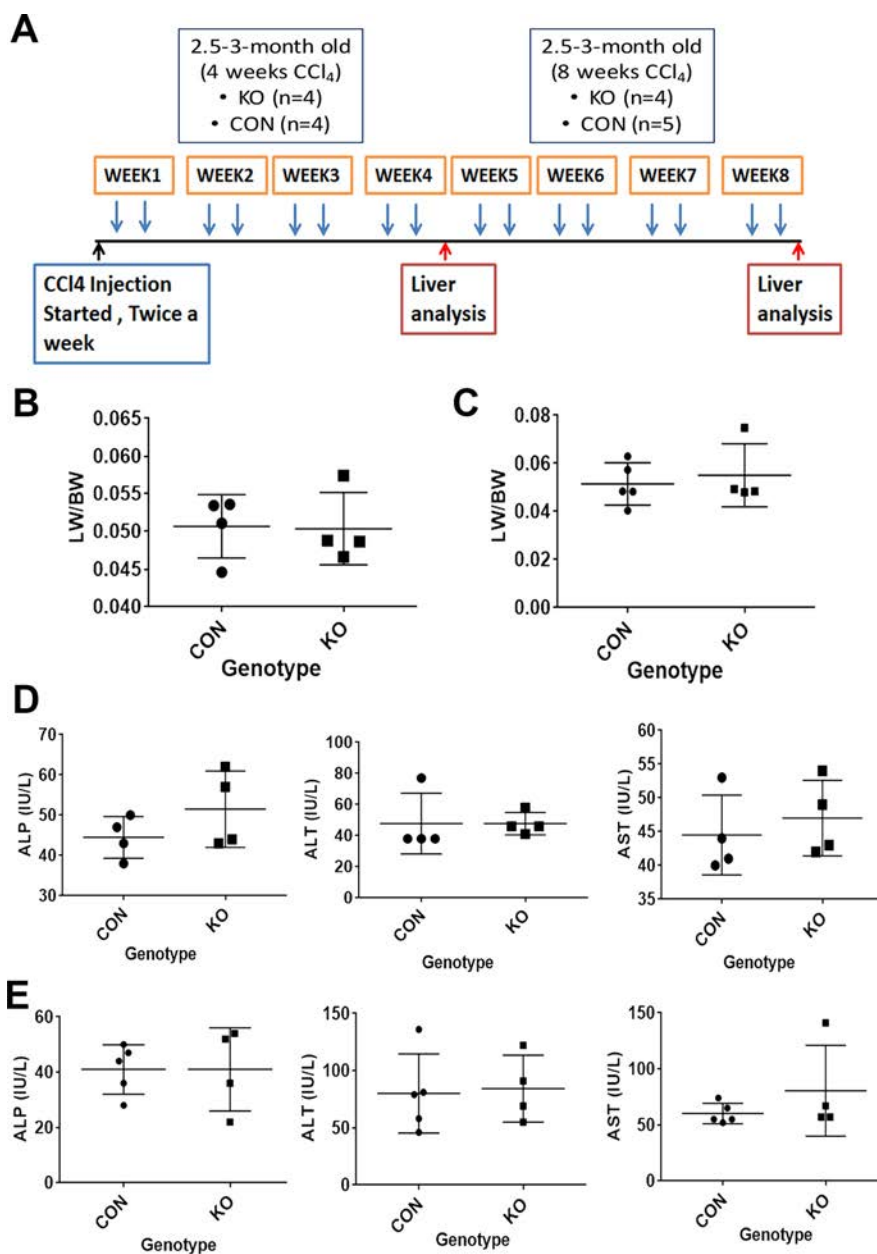


**Figure 7.** KO and CON mice exposed to CCl<sub>4</sub> twice weekly for 4 or 8 weeks assessed for biochemical injury. (A) Schematic showing age- and sex-matched 2.5- to 3-month old KO ( $n=4$ ) and CON ( $n=4$ ) mice exposed biweekly to IP injections of CCl<sub>4</sub> for 4 weeks or age- and sex-matched 2.5- to 3-month old KO ( $n=4$ ) and CON ( $n=5$ ) mice exposed biweekly to IP injections of CCl<sub>4</sub> for 8 weeks, at which time they were euthanized for serum and liver analysis. (B) No significant difference in liver weight-to-body weight ratio (LW/BW) between KO and WT after 4 weeks of biweekly CCl<sub>4</sub> treatment. (C) No significant difference in LW/BW between KO and WT after 8 weeks of biweekly CCl<sub>4</sub> treatment. (D) Four days after the last IP injection of CCl<sub>4</sub> in the 4-week group, KO and CON showed normal and comparable levels of ALP, ALT, and AST, with insignificant differences between the two groups. (E) Four days after the last IP injection of CCl<sub>4</sub> in the 8-week group, KO and CON also showed normal and comparable levels of ALP, ALT, and AST, with insignificant differences between the two groups.

CD45, and F4/80 did not reveal any notable differences in KO compared to CON (Fig. 10). Quantification of these stains confirmed the lack of significant differences between the two groups (Fig. 10). To determine the extent of fibrosis, we stained these tissues with Sirius

red, a marker of collagen deposition. Quantification of this stain also showed insignificant differences between KO and CON (Fig. 11A). IHC staining for desmin and  $\alpha$ -SMA was also comparable in KO and CON livers after 8 weeks of CCl<sub>4</sub> treatment, which was verified

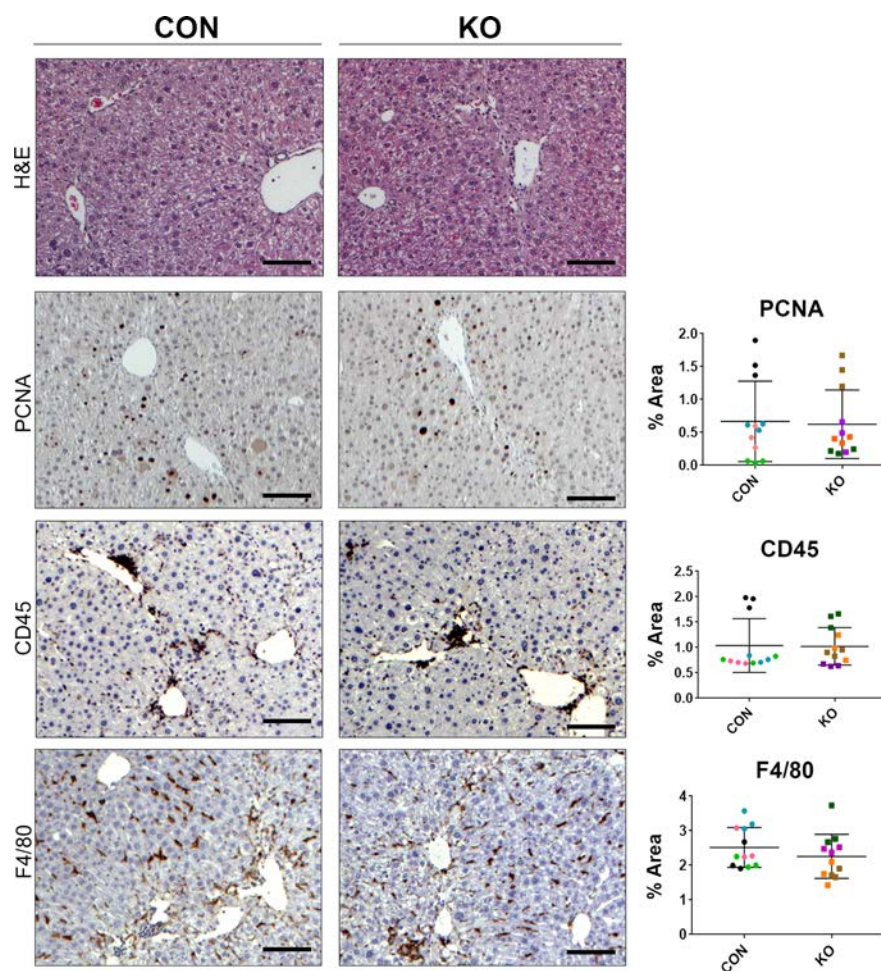


**Figure 8.** KO and CON mice exposed biweekly to  $\text{CCl}_4$  for 4 weeks showed comparable histological injury, repair, and inflammation. Representative sections from KO and CON after 4 weeks of  $\text{CCl}_4$  treatment show comparable histology by H&E of some inflammation, fibrosis, and necrosis. Also, representative staining on KO and CON at the same time for PCNA, CD45, and F4/80 show comparable numbers of hepatocytes in the S phase of the cell cycle, comparable immune cell infiltration, and similar numbers and distribution of macrophages, respectively. Quantification of each of these stains verified lack of significant differences between the two groups for any of these markers. Scale bar: 100  $\mu\text{m}$ .

by quantification as well (Fig. 11A). Likewise, protein levels of PDGFR $\alpha$ , PDGFR $\beta$ , desmin, and  $\alpha$ -SMA were comparable in KO and CON, by Western blot analysis (Fig. 11B). Thus, elimination of WIs, which prevents all Wnt secretion from HSCs, appears to be inconsequential in overall hepatic injury or fibrosis after 8 weeks of  $\text{CCl}_4$  treatment as well.

## DISCUSSION

The role of Wnt signaling in hepatic fibrosis has gained importance over the last decade<sup>10,36</sup>. It has been reported that the expression of Wnt, Fzd receptors, and coreceptors increases in culture-activated HSCs. For example, the Wnt ligands that have been reported to be upregulated in cultured rat HSC include Wnt3a<sup>36</sup>, Wnt10b<sup>36</sup>, Wnt4<sup>19,28,29,36</sup>, Wnt5a<sup>19,28,29,36</sup> and Wnt6<sup>28</sup>. Intriguingly,

in our current study, using primary HHSCs, treated with a known profibrogenic factor TGF- $\beta$ 1, we show increased mRNA expression of Wnt2, Wnt5a, and Wnt9a, but decreased mRNA of Wnt4, Wnt3a, and Wnt10b. The differences could be attributed to species and/or the varied strategies used to activate HSCs. Our study and others show that, during activation, HSCs do exhibit altered Wnt gene expression and hence may differentially secrete or respond to Wnt ligands in either an autocrine or paracrine manner. Interestingly, WLS, the gene encoding WIs protein, essential for all Wnts to be secreted from a cell, showed reduced expression following TGF- $\beta$ 1 treatment of HHSCs. This could imply an autocrine feedback loop in response to active Wnt signaling following TGF- $\beta$ 1 treatment, although more studies would be required to address the significance.

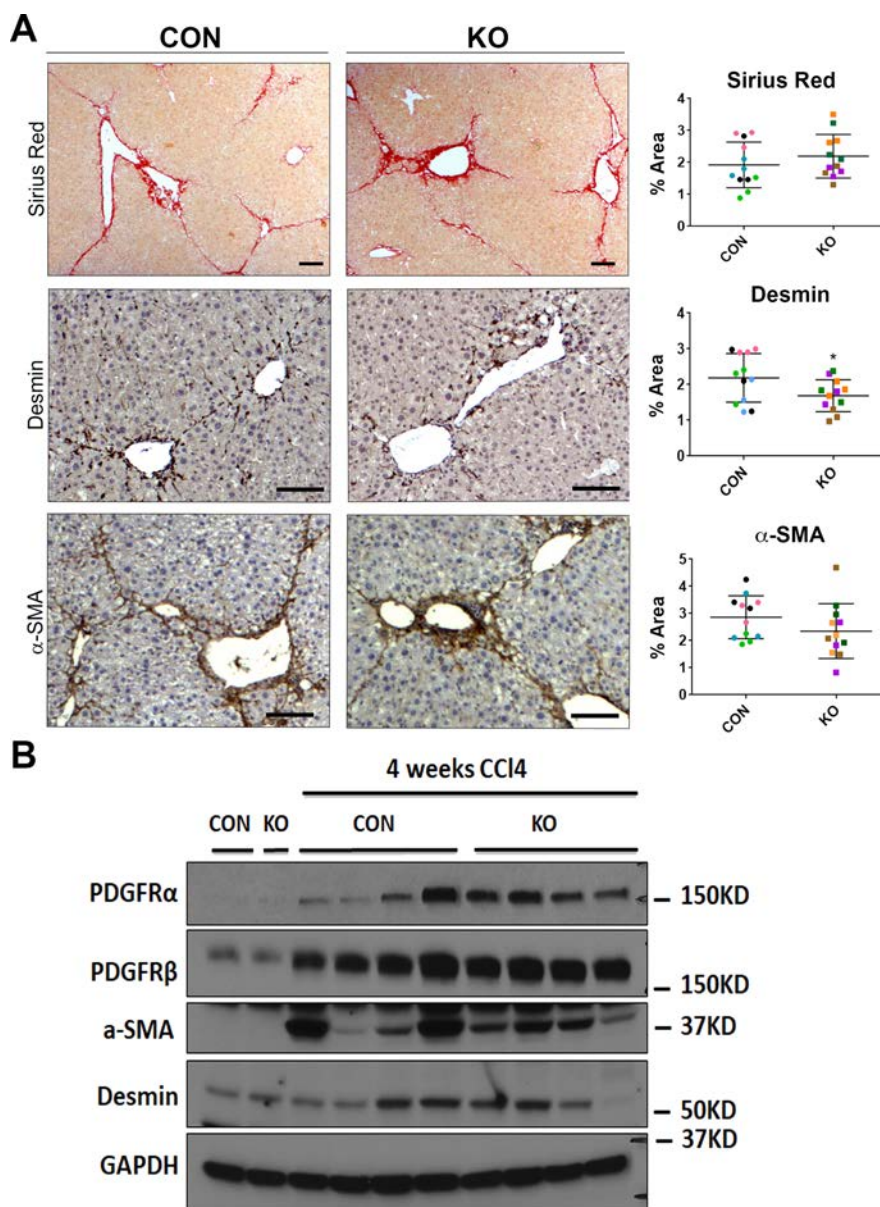


**Figure 9.** KO and CON mice exposed biweekly to CCl<sub>4</sub> for 4 weeks showed comparable HSC numbers, activated myofibroblasts, and extent of fibrosis. (A) Representative sections from KO and CON after 4 weeks of CCl<sub>4</sub> treatment show comparable Sirius red staining as well as immunostaining for desmin and α-SMA indicating similar fibrosis, number of HSCs, and activated myofibroblasts, respectively. Quantification of each of these stains verified lack of significant differences between the two groups for any of these markers. Scale bar: 100 μm. (B) Representative Western blot for markers of fibrosis showed comparably higher albeit somewhat variable desmin, α-SMA, PDGFR β, and PDGFR α levels in KO and CON after 4 weeks of CCl<sub>4</sub> treatment compared to their respective baseline controls. GAPDH was used as loading control.

Several additional studies have shown that abolishing Wnt signaling either *in vitro* or *in vivo* inhibits HSC activation to attenuate liver fibrosis<sup>20,22,27,36</sup>. We wanted to investigate if impeding all Wnt release from HSCs *in vivo* in two models of hepatic fibrosis would alter the course of the disease progression. To test this hypothesis, we employed conditional knockouts of Wls, which is specific and essential for Wnt secretion from a cell<sup>37,38</sup>. Previously

generated conditional KO using Wls-floxed mice have shown no compensation that allows Wnt secretion using any alternate molecule<sup>39-43</sup>. We have also used these mice to eliminate Wnt secretion from hepatocytes and macrophages in our previous study<sup>14,15,44</sup>. Knockout of Wls in HSCs was performed using *Lrat-cre*, a transgenic line shown to conditionally delete floxed genes from stellate cells at baseline as well as activated myofibroblasts in

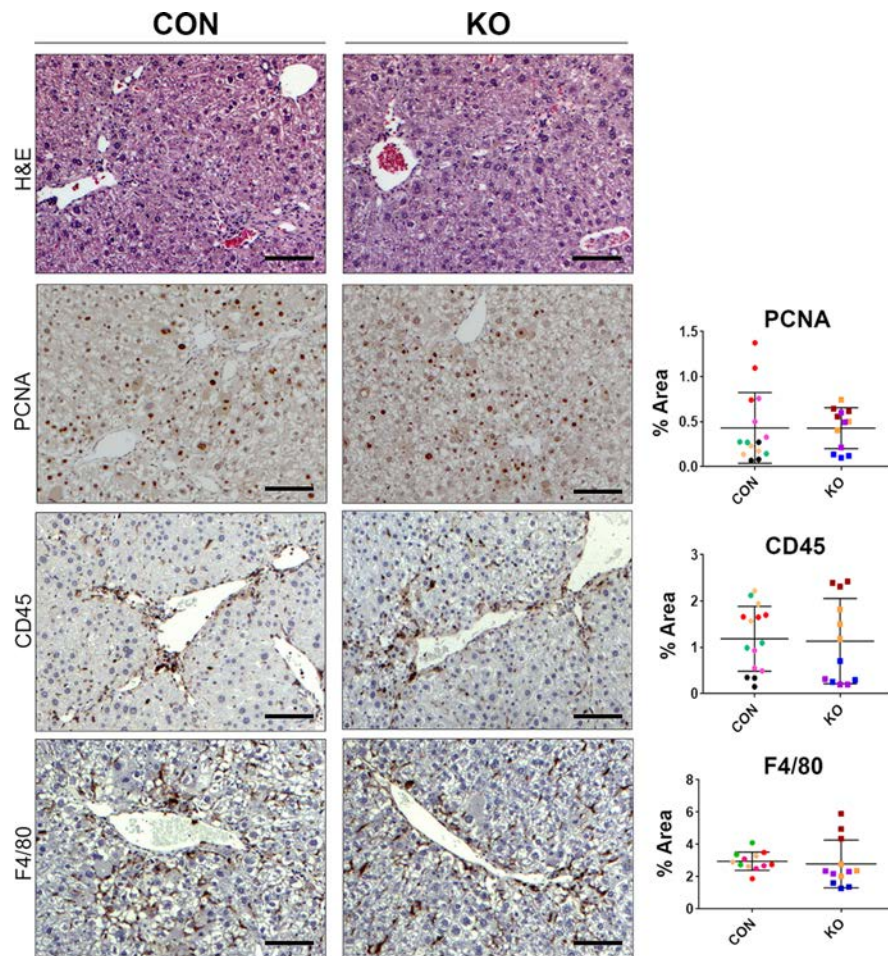


**Figure 10.** KO and CON mice exposed biweekly to  $\text{CCl}_4$  for 8 weeks showed comparable histological injury, repair, and inflammation. Representative sections from KO and CON after 8 weeks of  $\text{CCl}_4$  treatment show comparable histology by H&E of some inflammation, fibrosis, and necrosis. Also, representative staining on KO and CON at the same time for PCNA, CD45, and F4/80 show comparable numbers of hepatocytes in the S phase of the cell cycle, comparable immune cell infiltration, and similar numbers and distribution of macrophages, respectively. Quantification of each of these stains verified lack of significant differences between the two groups for any of these markers. Scale bar: 100  $\mu\text{m}$ .

both BDL and  $\text{CCl}_4$  models<sup>5</sup>. Indeed, we observed similar efficacy and hence validated the previous observation using fate tracing. In addition, we observed genetic deletion of WIs, loss of WIs mRNA expression, and EYFP<sup>+</sup> HSCs at baseline in KO mice; therefore, we posit that Wnt secretion is also abolished at baseline in KO mice. Nevertheless, mice that lacked WIs and hence Wnt secretion from HSCs did not exhibit any gross or microscopic liver phenotype. There was no decrease in basal LW/BW or baseline hepatocyte proliferation, which was reported in liver-specific  $\beta$ -catenin knockout mice as well as in liver-specific Wnt coreceptor, LRP5-6-double knockout mice<sup>13,14,45</sup>. Thus, Wnts that regulate postnatal hepatic growth, eventual liver weight, and hepatocyte proliferation through  $\beta$ -catenin activation are not likely originating from HSCs. Likewise, there was no disruption of metabolic zonation in the baseline KO mice seen as

continued expression of normal GS in pericentral hepatocytes, unlike the disruption observed in liver-specific  $\beta$ -catenin knockout and liver-specific LRP5-6-double knockout mice<sup>13,14</sup>. Therefore, it is likely that HSCs are not the primary cellular source of Wnts responsible for  $\beta$ -catenin activation in pericentral hepatocytes. However, as there is the possibility of a compensatory increase in secretion of Wnt ligands from other cells in the KO livers, we can only conclude that Wnt secretion by HSCs is dispensable for this process.

Having validated the efficacy of the HSC-specific *Lrat-Cre:WIs* mouse model at baseline, we next examined the role of Wnt secretion from HSCs in two independent fibrosis models. *Lrat-cre* has been previously shown to be effective in eliminating floxed genes in activated myofibroblasts in both BDL as well as  $\text{CCl}_4$  models of fibrosis since HSCs are a predominant contributor to the fibrosis

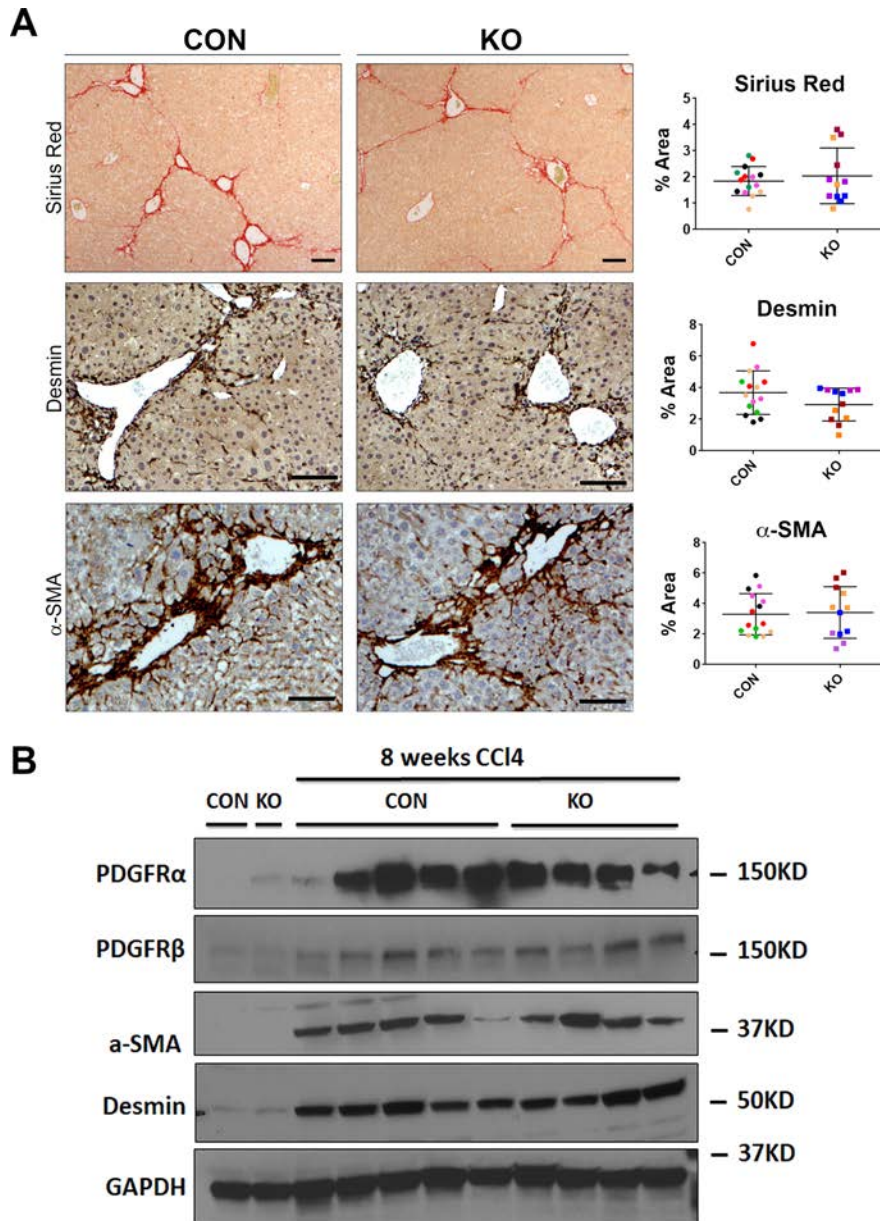


**Figure 11.** KO and CON mice exposed biweekly to CCl<sub>4</sub> for 8 weeks showed comparable HSC numbers, activated myofibroblasts, and extent of fibrosis. (A) Representative sections from KO and CON after 8 weeks of CCl<sub>4</sub> treatment show comparable Sirius red staining as well as immunostaining for desmin and  $\alpha$ -SMA indicating similar fibrosis, number of HSCs, and activated myofibroblasts, respectively. Quantification of each of these stains verified lack of significant differences between the two groups for any of these markers. Scale bar: 100  $\mu$ m. (B) Representative Western blot for markers of fibrosis showed comparably higher albeit somewhat variable desmin,  $\alpha$ -SMA, PDGFR  $\alpha$ , and PDGFR  $\beta$  levels in KO and CON after 8 weeks of CCl<sub>4</sub> treatment compared to their respective baseline controls. GAPDH was used as loading control.

process in both models<sup>5,46</sup>. To our surprise, KO mice showed the same levels of HSC activation and extent of liver fibrosis as CON following 7 days of BDL as well as 4 or 8 weeks of biweekly CCl<sub>4</sub> injection. One obvious explanation of these negative results is that Wnt secretion from HSCs does not play any significant role in development or progression of hepatic fibrosis, especially since

we did not find appreciable differences in fibrosis histologically or via limited protein analysis of whole liver lysates. Only in BDL model did we observe a modest but consistent decrease in PDGFR  $\alpha$  and PDGFR  $\beta$  levels in KO, both of which are critical for HSC activation, proliferation, and migration in various forms of hepatobiliary injury<sup>33,47,48</sup>. This decrease may be attributable to the lack

of an autocrine Wnt signal that maintains PDGFR expression in HSCs, which is effected by the HSC-specific Wls KO.

As Wnt signaling is required for HSC activation and fibrosis, and the HSC-specific Wls KO affects the ability of HSCs to secrete Wnt ligands, but does not alter their ability to respond to Wnts, it is possible that other cellular sources of Wnts are responsible for HSC activation in our model. It has been reported that hepatocytes, biliary epithelial cells, sinusoidal epithelial cells, Kupffer cells in addition to HSCs all express Wnt genes in a normal liver<sup>49</sup>. Also, overexpression of Wnt ligands, including Wnt10b<sup>17</sup>, Wnt12<sup>17</sup>, Wnt2<sup>17</sup>, Wnt13<sup>17,18</sup>, and Wnt5a<sup>17,26</sup>, has been reported in diseased liver. It is possible that Wnt ligands from any of these cell populations could activate Wnt signaling in HSCs. Nevertheless, as stated above for baseline liver biology, we can definitively say that secretion of Wnt ligands by HSCs is expendable for HSC activation, hepatic fibrosis, and injury–repair processes. Further studies that require cell separation and analysis of Wnt expression may be essential to address compensation of Wls loss from HSCs both at baseline and after injury.

An alternative explanation for the lack of differences in the extent of fibrosis and comparable myofibroblast activation could be that deletion of Wls from HSCs eliminated secretion of both profibrotic and antifibrotic Wnt ligands to negate any overall effect. The predominant point of view from a substantial amount of literature is that canonical Wnt signaling along with Wnt5a signaling are mostly profibrotic<sup>20–31,36</sup>. However, one study also showed that activation of canonical Wnt signaling by TWS119 exhibited an antifibrotic phenotype in HSCs<sup>19</sup>. Thus, a possibility exists that blocking all Wnt release from HSCs neutralizes the profibrotic and antifibrotic effect of Wnt signaling thus leading to an equivocal fibrotic response between the KO and CON. Thus, selective conditional deletion of specific Wnt genes especially the ones notably upregulated in HSCs after profibrogenic signals, such as Wnt2, Wnt5a, and Wnt9a, may be important to address their overall impact on HSC biology and development of fibrosis.

*ACKNOWLEDGMENTS: Supported in part by NIH grants IR01DK62277, IR01DK100287, R01CA204586, Research Grant No: I# 0050815 from Abbvie Pharmaceuticals and an Endowed Chair for Experimental Pathology (S.P.M.). Dr. Monga is a consultant and has a research grant from Abbvie and is a consultant for Dicerna. Dr. Steven England is an employee of Abbvie.*

## REFERENCES

- Bataller R, Brenner DA. Liver fibrosis. *J Clin Invest*. 2005;115(2):209–18.
- Gressner AM, Weiskirchen R. 2006. Modern pathogenetic concepts of liver fibrosis suggest stellate cells and TGF- as major players and therapeutic targets. *J Cell Mol Med*. 2006;10(1):76–99.
- Friedman SL. Hepatic stellate cells: Protean, multifunctional, and enigmatic cells of the liver. *Physiol Rev*. 2008; 88(1):125–72.
- Iwaisako K, Jiang C, Zhang M, Cong M, Moore-Morris TJ, Park TJ, Liu X, Xu J, Wang P, Paik Y-H, et al. Origin of myofibroblasts in the fibrotic liver in mice. *Proc Natl Acad Sci USA* 2014;111(32):E3297–305.
- Mederacke I, Hsu CC, Troeger JS, Huebener P, Mu X, Dapito DH, Pradere J-P, Schwabe RF. Fate-tracing reveals hepatic stellate cells as dominant contributors to liver fibrosis independent of its etiology. *Nat Commun*. 2013;4: 2823.
- Pellicoro A, Ramachandran P, Iredale JP, Fallowfield JA. Liver fibrosis and repair: Immune regulation of wound healing in a solid organ. *Nat Rev Immunol*. 2014;14:181.
- Higashi T, Friedman SL, Hoshida Y. Hepatic stellate cells as key target in liver fibrosis. *Adv Drug Delivery Rev*. 2017;121(Suppl C):27–42.
- Moreira RK. Hepatic stellate cells and liver fibrosis. *Arch Pathol Lab Med*. 2007;131(11):1728–34.
- Wallace MC, Friedman SL, Mann DA. Emerging and disease-specific mechanisms of hepatic stellate cell activation. *Semin Liver Dis*. 2015;35(02):107–18.
- Monga SP. B-catenin signaling and roles in liver homeostasis, injury, and tumorigenesis. *Gastroenterology* 2015; 148(7):1294–310.
- Veeman MT, Axelrod JD, Moon RT. A second canon: Functions and mechanisms of  $\beta$ -catenin-independent Wnt signaling. *Dev Cell*. 2003;5(3):367–77.
- Benhamouche S, Decaens T, Godard C, Chambrey R, Rickman DS, Moinard C, Vasseur-Cognet M, Kuo CJ, Kahn A, Perret C, et al. Apc tumor suppressor gene is the “zonation-keeper” of mouse liver. *Dev Cell*. 2006;10(6): 759–70.
- Tan X, Behari J, Cieply B, Michalopoulos GK, Monga SP. Conditional deletion of beta-catenin reveals its role in liver growth and regeneration. *Gastroenterology* 2006; 131(5):1561–72.
- Yang J, Mowry LE, Nejak-Bowen KN, Okabe H, Diegel CR, Lang RA, Williams BO, Monga SP. Beta-catenin signaling in murine liver zonation and regeneration: A Wnt-Wnt situation! *Hepatology* 2014;60(3):964–76.
- Preziosi M, Okabe H, Poddar M, Singh S, Monga SP. Endothelial Wnts regulate beta-catenin signaling in murine liver zonation and regeneration: A sequel to the Wnt-Wnt situation. *Hepatology* 2018;2(7):845–60.
- Wang B, Zhao L, Fish M, Logan CY, Nusse R. Self-renewing diploid axin2(+) cells fuel homeostatic renewal of the liver. *Nature* 2015;524(7564):180–5.
- Shackel N, McGuinness P, Abbott C, Gorrell M, McCaughan G. Identification of novel molecules and pathogenic pathways in primary biliary cirrhosis: CDNA array analysis of intrahepatic differential gene expression. *Gut* 2001;49(4): 565–76.
- Tanaka A, Leung PSC, Kenny TP, Au-Young J, Prindiville T, Coppel RL, Ansari AA, Gershwin ME. Genomic analysis of differentially expressed genes in liver and biliary epithelial cells of patients with primary biliary cirrhosis. *J Autoimmun*. 2001;17(1):89–98.
- Kordes C, Sawitzka I, Häussinger D. Canonical Wnt signaling maintains the quiescent stage of hepatic stellate cells. *Biochem Biophys Res Commun*. 2008;367(1):116–23.

20. Li W, Zhu C, Li Y, Wu Q, Gao R. Mest attenuates CCl<sub>4</sub>-induced liver fibrosis in rats by inhibiting the Wnt/ $\beta$ -catenin signaling pathway. *Gut Liver* 2014;8(3):282–91.
21. Myung SJ, Yoon J-H, Gwak G-Y, Kim W, Lee J-H, Kim KM, Shin CS, Jang JJ, Lee S-H, Lee S-M, et al. Wnt signaling enhances the activation and survival of human hepatic stellate cells. *FEBS Lett*. 2007;581(16):2954–8.
22. Osawa Y, Oboki K, Imamura J, Kojika E, Hayashi Y, Hishima T, Saibara T, Shibasaki F, Kohara M, Kimura K. Inhibition of cyclic adenosine monophosphate (cAMP)-response element-binding protein (CREB)-binding protein (CBP)/ $\beta$ -catenin reduces liver fibrosis in mice. *EBioMedicine* 2015;2(11):1751–8.
23. Yin X, Yi H, Wang L, Wu W, Wu X, Yu L. RSPOs facilitated HSC activation and promoted hepatic fibrogenesis. *Oncotarget* 2016;7(39):63767–78.
24. Yin X, Yi H, Wu W, Shu J, Wu X, Yu L. R-spondin2 activates hepatic stellate cells and promotes liver fibrosis. *Dig Dis Sci*. 2014;59(10):2452–61.
25. Zhu N-L, Wang J, Tsukamoto H. The Necdin-Wnt pathway causes epigenetic peroxisome proliferator-activated receptor  $\alpha$  repression in hepatic stellate cells. *J Biol Chem*. 2010;285(40):30463–71.
26. Beljaars L, Daliri S, Dijkhuizen C, Poelstra K, Gosens R. Wnt-5a regulates TGF- $\beta$ -related activities in liver fibrosis. *Am J Physiol Gastrointest Liver Physiol*. 2017;312(3):G219–27.
27. Chatani N, Kamada Y, Kizu T, Ogura S, Furuta K, Egawa M, Hamano M, Ezaki H, Kiso S, Shimono A, et al. Secreted frizzled-related protein 5 (Sfrp5) decreases hepatic stellate cell activation and liver fibrosis. *Liver Int*. 2015;35(8):2017–26.
28. Corbett L, Mann J, Mann DA. Non-canonical Wnt predominates in activated rat hepatic stellate cells, influencing HSC survival and paracrine stimulation of Kupffer cells. *PLoS One* 2015;10(11):e0142794.
29. Jiang F, Parsons CJ, Stefanovic B. Gene expression profile of quiescent and activated rat hepatic stellate cells implicates Wnt signaling pathway in activation. *J Hepatol*. 2006;45(3):401–9.
30. Rashid ST, Humphries JD, Byron A, Dhar A, Askari JA, Selley JN, Knight D, Goldin RD, Thursz M, Humphries MJ. Proteomic analysis of extracellular matrix from the hepatic stellate cell line LX-2 identifies CYR61 and Wnt-5a as novel constituents of fibrotic liver. *J Proteome Res*. 2012;11(8):4052–64.
31. Xiong W-J, Hu L-J, Jian Y-C, Wang L-J, Jiang M, Li W, He Y. Wnt5a participates in hepatic stellate cell activation observed by gene expression profile and functional assays. *World J Gastroenterol*. 2012;18(15):1745–52.
32. Gabriel A, Kuddus RH, Rao AS, Watkins WD, Gandhi CR. Superoxide-induced changes in endothelin (ET) receptors in hepatic stellate cells. *J Hepatol*. 1998;29(4):614–27.
33. Kikuchi A, Pradhan-Sundt T, Singh S, Nagarajan S, Loizos N, Monga SP. Platelet-derived growth factor receptor alpha contributes to human hepatic stellate cell proliferation and migration. *Am J Pathol*. 2017;187(10):2273–87.
34. Borkham-Kamphorst E, Kovalenko E, van Roeyen CRC, Gassler N, Bomble M, Ostendorf T, Floege J, Gressner AM, Weiskirchen R. Platelet-derived growth factor isoform expression in carbon tetrachloride-induced chronic liver injury. *Lab Invest*. 2008;88:1090.
35. Hayes BJ, Riehle KJ, Shimizu-Albergine M, Bauer RL, Hudkins KL, Johansson F, Yeh MM, Mahoney WM Jr, Yeung RS, Campbell JS. Activation of platelet-derived growth factor receptor alpha contributes to liver fibrosis. *PLoS One* 2014;9(3):e92925.
36. Cheng JH, She H, Han YP, Wang J, Xiong S, Asahina K, Tsukamoto H. Wnt antagonism inhibits hepatic stellate cell activation and liver fibrosis. *Am J Physiol Gastrointest Liver Physiol*. 2008;294(1):G39–49.
37. Bänziger C, Soldini D, Schütt C, Zipperlen P, Hausmann G, Basler K. Wntless, a conserved membrane protein dedicated to the secretion of Wnt proteins from signaling cells. *Cell* 2006;125(3):509–22.
38. Bartscherer K, Pelte N, Ingelfinger D, Boutros M. Secretion of Wnt ligands requires Evi, a conserved transmembrane protein. *Cell* 2006;125(3):523–33.
39. Carpenter AC, Rao S, Wells JM, Campbell K, Lang RA. Generation of mice with a conditional null allele for Wntless. *Genesis* 2010;48(9):554–8.
40. Carpenter AC, Smith AN, Wagner H, Cohen-Tayar Y, Rao S, Wallace V, Ashery-Padan R, Lang RA. Wnt ligands from the embryonic surface ectoderm regulate ‘bimetallic strip’ optic cup morphogenesis in mouse. *Development* 2015;142(5):972–82.
41. Irvine KM, Clouston AD, Gadd VL, Miller GC, Wong WY, Melino M, Maradana MR, MacDonald K, Lang RA, Sweet MJ, et al. Deletion of Wntless in myeloid cells exacerbates liver fibrosis and the ductular reaction in chronic liver injury. *Fibrogenesis Tissue Repair* 2015;8:19.
42. Muley A, Odaka Y, Lewkowich IP, Vemuraju S, Yamaguchi TP, Shawber C, Dickie BH, Lang RA. Myeloid Wnt ligands are required for normal development of dermal lymphatic vasculature. *PLoS One* 2017;12(8):e0181549.
43. Snowball J, Ambalavanan M, Cornett B, Lang R, Whitsett J, Sinner D. Mesenchymal Wnt signaling promotes formation of sternum and thoracic body wall. *Dev Biol*. 2015;401(2):264–75.
44. Preziosi M, Poddar M, Singh S, Monga SP. Hepatocyte Wnts are dispensable during diethylnitrosamine and carbon tetrachloride-induced injury and hepatocellular cancer. *Gene Expr*. 2018;18(3):209–19.
45. Apte U, Zeng G, Thompson MD, Muller P, Micsenyi A, Cieply B, Kaestner KH, Monga SP. Beta-catenin is critical for early postnatal liver growth. *Am J Physiol Gastrointest Liver Physiol*. 2007;292(6):G1578–85.
46. Lua I, Li Y, Zagory JA, Wang KS, French SW, Sevigny J, Asahina K. Characterization of hepatic stellate cells, portal fibroblasts, and mesothelial cells in normal and fibrotic livers. *J Hepatol*. 2016;64(5):1137–46.
47. Kikuchi A, Monga SP. PDGFR $\alpha$  in liver pathophysiology: Emerging roles in development, regeneration, fibrosis, and cancer. *Gene Expr*. 2015;16(3):109–27.
48. Kocabayoglu P, Lade A, Lee YA, Dragomir AC, Sun X, Fiel MI, Thung S, Aloman C, Soriano P, Hoshida Y, et al. Beta-PDGF receptor expressed by hepatic stellate cells regulates fibrosis in murine liver injury, but not carcinogenesis. *J Hepatol*. 2015;63(1):141–7.
49. Zeng G, Awan F, Otruba W, Muller P, Apte U, Tan X, Gandhi C, Demetris AJ, Monga SPS. Wnt $\beta$  in liver: Expression of Wnt and frizzled genes in mouse. *Hepatology* 2007;45(1):195–204.